

Self-association-driven transition of the β -peptidic H12 helix to the H18 helix

Éva Szolnoki,^a Anasztázia Hetényi,^b Tamás A. Martinek,^{*a} Zsolt Szakonyi^a Ferenc Fülöp^a

^aInstitute of Pharmaceutical Chemistry, University of Szeged, Eötvös u. 6., H-6720 Szeged, Hungary,

^bDepartment of Medical Chemistry, University of Szeged, H-6720 Szeged, Dóm tér 8., Hungary

martinek@pharm.u-szeged.hu

TABLE OF CONTENTS

Materials and Methods	S2
Fig. S1 TOCSY (top) and ROESY (bottom) spectra of 1 in [D ₆]DMSO.	S3
Fig. S2 TOCSY (top) and ROESY (bottom) spectra of 2 in [D ₆]DMSO.	S4
Fig. S3 TOCSY (top) and ROESY (bottom) spectra of 3 in [D ₆]DMSO.	S5
Fig. S4 TOCSY (top) and ROESY (bottom) spectra of 4 in [D ₆]DMSO.	S6
Fig. S5 TOCSY (top) and ROESY (bottom) spectra of 5 in [D ₆]DMSO.	S7
Fig. S6 TOCSY (top) and ROESY (bottom) spectra of 1 in CD ₃ OH.	S8
Fig. S7 TOCSY (top) and ROESY (bottom) spectra of 2 in CD ₃ OH.	S9
Fig. S8 TOCSY (top) and ROESY (bottom) spectra of 3 in CD ₃ OH.	S10
Fig. S9 TOCSY (top) and ROESY (bottom) spectra of 4 in CD ₃ OH.	S11
Fig. S10 TOCSY (top) and ROESY (bottom) spectra of 5 in CD ₃ OH.	S12
Fig. S11 Long-range NOE interactions for 3-5 in [D ₆]DMSO.	S13
Fig. S12 Time dependence of the NH/ND exchange for 5 in CD ₃ OD.	S13
Fig. S13 Diagnostic head-to-tail cross-peaks in the ROESY spectrum of 5 in CD ₃ OH.	S14
Fig. S14 TEM image of 5 .	S14
Fig. S15 ln(I/I ₀) vs. G ² for 3 .	S15
Fig. S16 ln(I/I ₀) vs. G ² for 4 .	S15
Fig. S17 ln(I/I ₀) vs. G ² for 5 .	S15
Fig. S18 Negative temperature gradients of the chemical shifts for the NH protons in 1-5 in [D ₆]DMSO.	S16
Fig. S19 <i>Ab initio</i> geometries of 1-3 .	S17
Fig. S20 HPLC chromatogram of purified 1 .	S17
Fig. S21 HPLC chromatogram of purified 2 .	S18
Fig. S22 HPLC chromatogram of purified 3 .	S18
Fig. S23 HPLC chromatogram of purified 4 .	S18
Fig. S24 HPLC chromatogram of purified 5 .	S18
Fig. S25 ESI-MS spectrum of 1 .	S19
Fig. S26 ESI-MS spectrum of 2 .	S19
Fig. S27 ESI-MS spectrum of 3 .	S20
Fig. S28 ESI-MS spectrum of 4 .	S20
Fig. S29 ESI-MS spectrum of 5 .	S21
Fig. S30 IR spectrum of 1 .	S21
Fig. S31 IR spectrum of 2 .	S21
Fig. S32 IR spectrum of 3 .	S22
Fig. S33 IR spectrum of 4 .	S22
Fig. S34 IR spectrum of 5 .	S22
Fig. S35 UV spectra of 1-5 , a-e respectively.	S23
Table S1 Signal assignments of the backbone for 1-3 in [D ₆]DMSO.	S23
Table S2 Signal assignments of the backbone for 4-5 in [D ₆]DMSO.	S24
Table S3 Signal assignments of the backbone for 1-3 in CD ₃ OH.	S24
Table S4 Signal assignments of the backbone for 4-5 in CD ₃ OH.	S25
Table S5 ³ J (NH _i -C ^β H _i) values in [D ₆]DMSO (Hz).	S25
Table S6 ³ J (NH _i -C ^β H _i) values in CD ₃ OH (Hz).	S25
Table S7 Measured aggregation numbers (N) for 3-5 .	S26
Gaussian ref	S26

Materials and Methods

Peptide synthesis

Foldamers **1-5** were synthesized by using a standard solid-phase technique involving 9H-fluoren-9-ylmethoxycarbonyl (Fmoc) chemistry. The peptide chains were elongated on TentaGel R RAM resin (0.19 mmol g⁻¹) and the syntheses were carried out manually on a 0.2 mmol scale. Couplings were performed with HATU/DIPEA, without difficulties. The peptide sequences were cleaved from the resin with 95% TFA and 5% H₂O at room temperature for 3 h. This method leads to lactone side-products because of the C-terminal β³-homoserine residue. The TFA was then removed, and the resulting free peptides were solubilized in aqueous acetic acid (10%), filtered off and lyophilized. The crude peptides were investigated by RP-HPLC, using a Phenomenex C18 column (4.6 × 250 mm) for **1-4** and a Phenomenex C4 column (4.6 × 250 mm) for **5**. The solvent system used was TFA (0.1%) in water (A), TFA (0.1%) and acetonitrile (80%) in water (B), gradient: 5%→100% B during 35 min, flow rate 1.2 mL min⁻¹, detection at 206 nm. The above peptides were purified on an HPLC system on a Phenomenex C18 column (10 × 250 mm) and a Phenomenex C4 column (10 × 250 mm). The appropriate fractions were pooled and lyophilized. The purified peptides were characterized by mass spectrometry with an Agilent 1100 LC-MSD trap mass spectrometer equipped with an electrospray ion source. The spectra were run in positive ionization mode with scanning in the m/z interval 100-2200. The measured molecular weights were as follows: **1** m/z (M+H) = 917.5, **2** m/z (M+H) = 853.5, **3** m/z (M+H) = 981.7, **4** m/z (M+H) = 1146.7, **5** m/z (M+H) = 1311.8.

NMR experiments

NMR measurements were performed on a Bruker Avance III 600 MHz spectrometer with a multinuclear probe with a z-gradient coil in 0.5 – 1 mM CD₃OH at temperatures between 283 and 310 K, and in [D₆]DMSO solutions between 298 – 323 K. The ROESY measurements were performed with the WATERGATE solvent suppression scheme. For the ROESY spinlock, mixing times of 225 and 400 ms were used; the number of scans was 64. The TOCSY measurements were made with homonuclear Hartman-Hahn transfer with the MLEV17 sequence, with a mixing time of 80 ms; the number of scans was 32. For all the 2D spectra, 2024 time domain points and 512 increments were applied. The processing was carried out by using a cosine-bell window function, with single zero filling and automatic baseline correction. The DOSY (PFGSE) NMR measurements were performed by using the stimulated echo and longitudinal eddy current delay (LED) sequence with water suppression. A time of 2 ms was used for the dephasing/refocusing gradient pulse length (δ), and 250 ms for the diffusion delay (Δ). The gradient strength was changed quadratically (from 5% to 60-95% of the maximum value B-AFPA 10 A gradient amplifier), and the number of steps was 16. Each measurement was run with 64 scans and 2K time domain points. For the processing, an exponential window function and single zero filling were applied. During the diffusion measurements, the temperature fluctuation was less than 0.1 K. Prior to the NMR scans, all the samples were equilibrated for 30 min. DOSY spectra were processed and evaluated by using the exponential fit implemented in Topspin 3.0. The aggregation numbers were calculated from the Stokes-Einstein equation and TMS was utilized as an external volume standard.

ECD measurements

ECD spectra were measured on a Jasco J815 spectrometer at 25 °C in a 0.02 cm cell. The baseline spectrum recorded with the solvent only was subtracted from the raw data. The concentration of the sample solutions was 1 mM and for the concentration-dependent measurements the concentration of the sample solution series was 25 μM – 1 mM in CD₃OH. Ten spectra were accumulated for each sample. Molar ellipticity, [θ], is given in deg cm² dmol⁻¹. The data were normalized for the oligomer concentration and the number of chromophores.

IR measurements

FT-IR spectra were recorded on a Perkin-Elmer Spectrum 100 instrument. Microanalyses were performed on a Perkin-Elmer 2400 elemental analyser.

UV measurements

The UV spectra were measured by a spectrometer UV-1800 in the range 190–250 nm in cells with optical path 1 cm. The data obtained were exported in text files. The correlation coefficients were determined by numerical analyses of the raw spectral data.

Molecular mechanics calculations

Molecular mechanical simulations were carried out in the Molecular Operating Environment (MOE) of the Chemical Computing Group. For the energy calculations, the MMFF94x force field was used, without a cut-off for van der Waals and Coulomb interactions, and the distance-dependent dielectric constant (ε_r) was set to ε = 1.8 (corresponding to CH₃OH). For the protonated backbones, the implicit water model of GB/VI (Generalized Born) was applied. The conformational sampling was carried out by using the hybrid Monte Carlo (MC) – molecular dynamics (MD) simulation (as implemented in MOE) at 300 K with a random MC sampling step after every 10 MD steps. The MC-MD simulation was run with a step size of 2 fs for 20 ns, and the conformations were saved after every 1000 MD steps, which resulted in 10⁴ structures. For the NMR restrained simulation, the upper distance limits were calculated by using the isolated spin pair approximation and classified by following the standard method (strong: 2.5 Å, medium 3.5 Å, and weak 5 Å). The lower limit was set to 1.8 Å. Restraints were applied as a flat-bottomed quadratic penalty term with a force constant of 5 kcal Å⁻². The final conformations were minimized to a gradient of 0.05 kcal mol⁻¹ and the minimization was applied in a cascade manner, using the steepest-descent, conjugate gradient and truncated

Newton algorithm.

Ab initio calculations.

The optimizations were carried out in two steps with the Gaussian 09 program: first by using the HF/3-21G basis set, and then by using density-functional theory at the B3LYP/6-311G** level with a default setup. For the protonated models, the level of B3LYP/6-311* with the PCM methanol model was utilized.

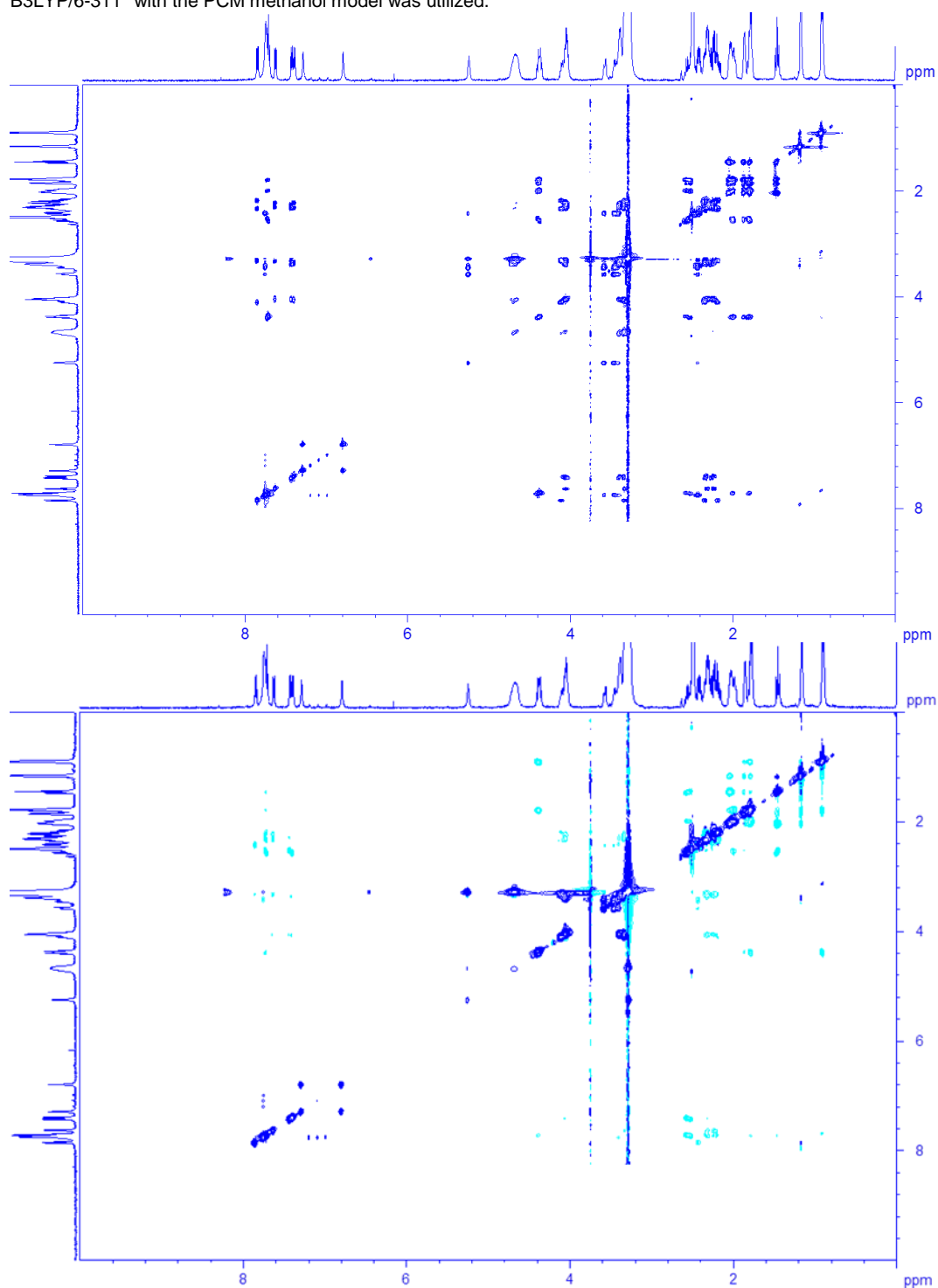


Fig. S1 TOCSY (top) and ROESY (bottom) spectra of **1**. Conditions: [D₆]DMSO, 1 mM, 305 K.

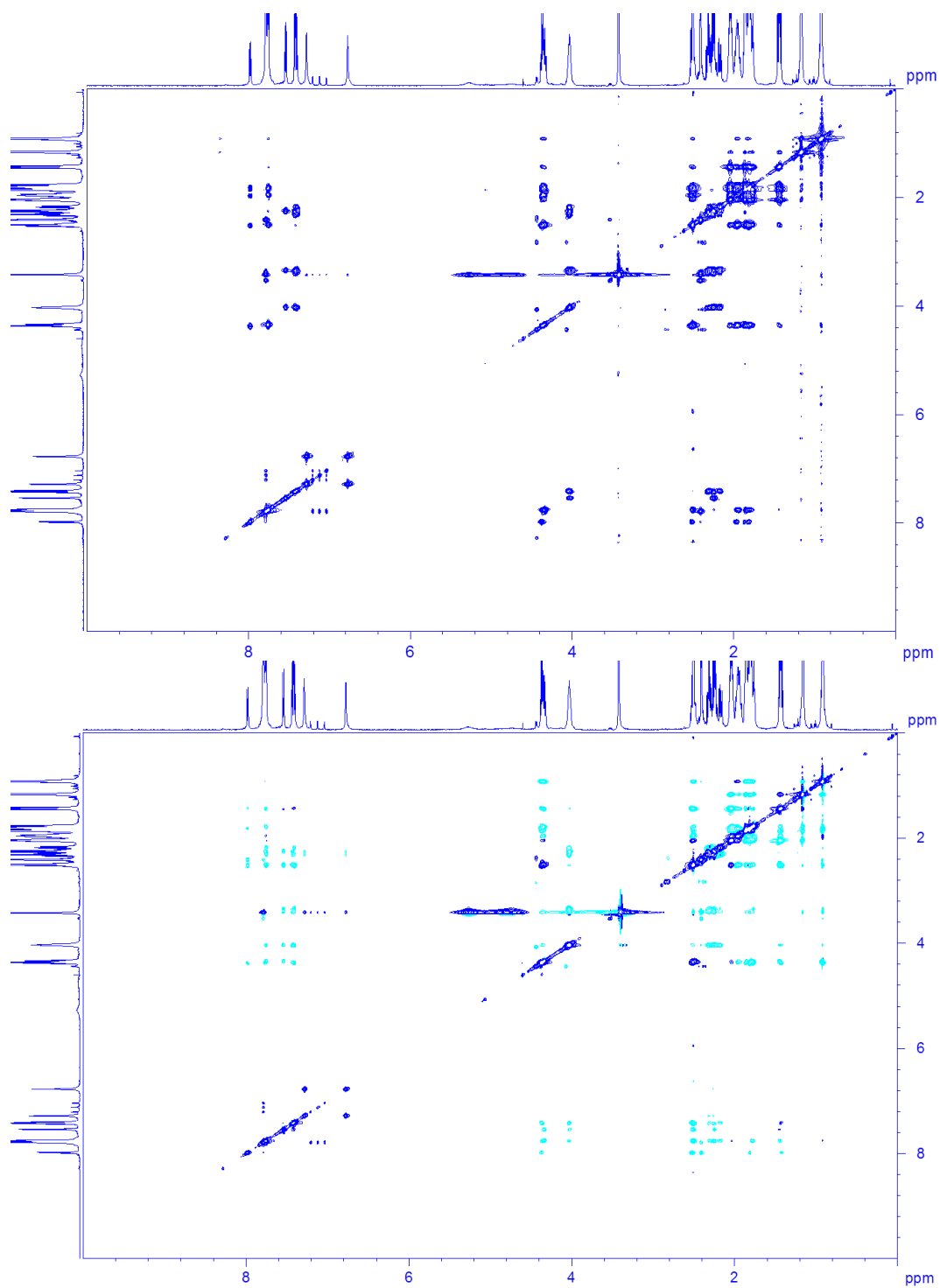


Fig. S2 TOCSY (top) and ROESY (bottom) spectra of **2**. Conditions: [D₆]DMSO, 1 mM, 310 K.

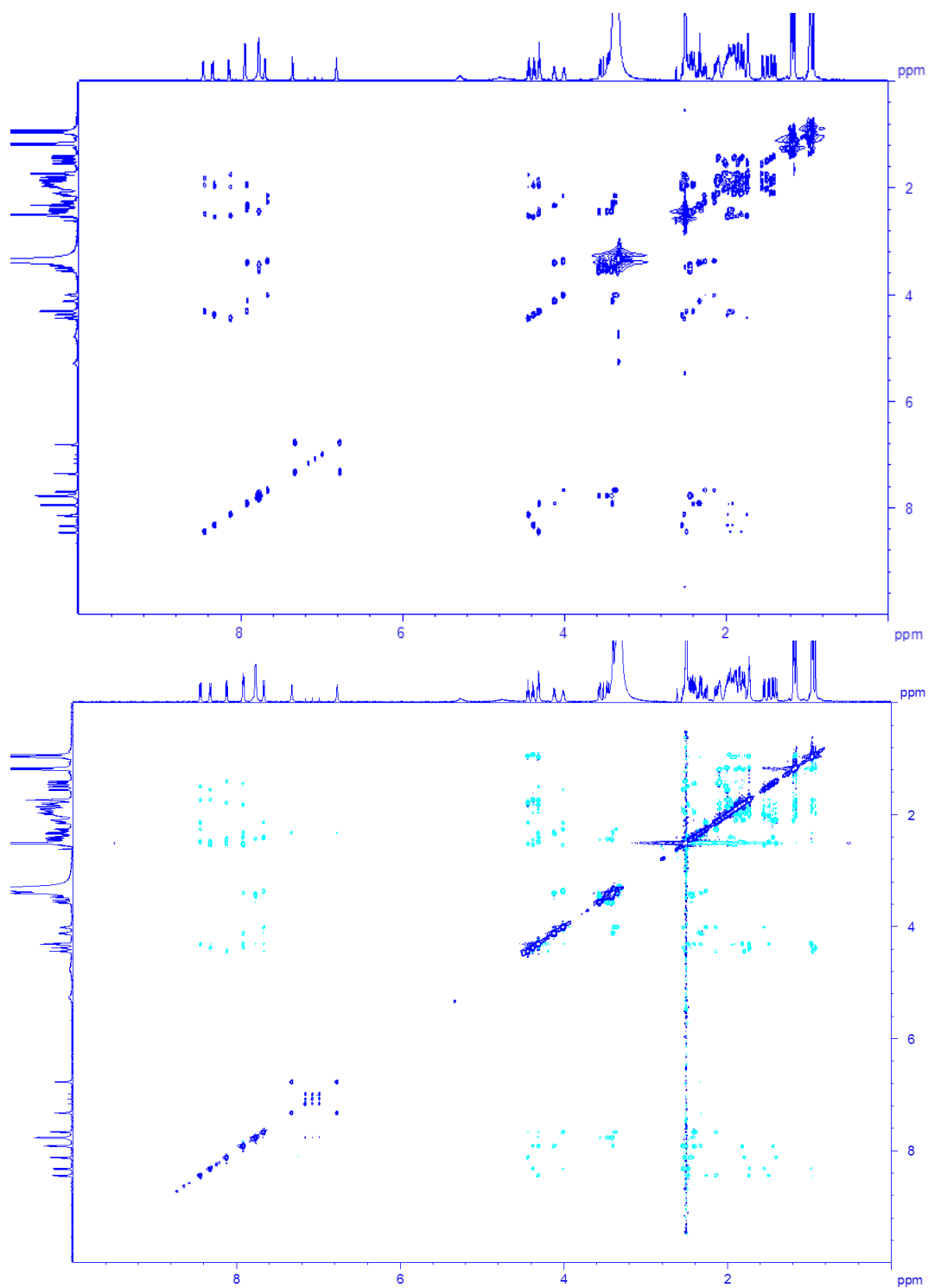


Fig. S3 TOCSY (top) and ROESY (bottom) spectra of **3**. Conditions: $[D_6]DMSO$, 1 mM, 303 K.

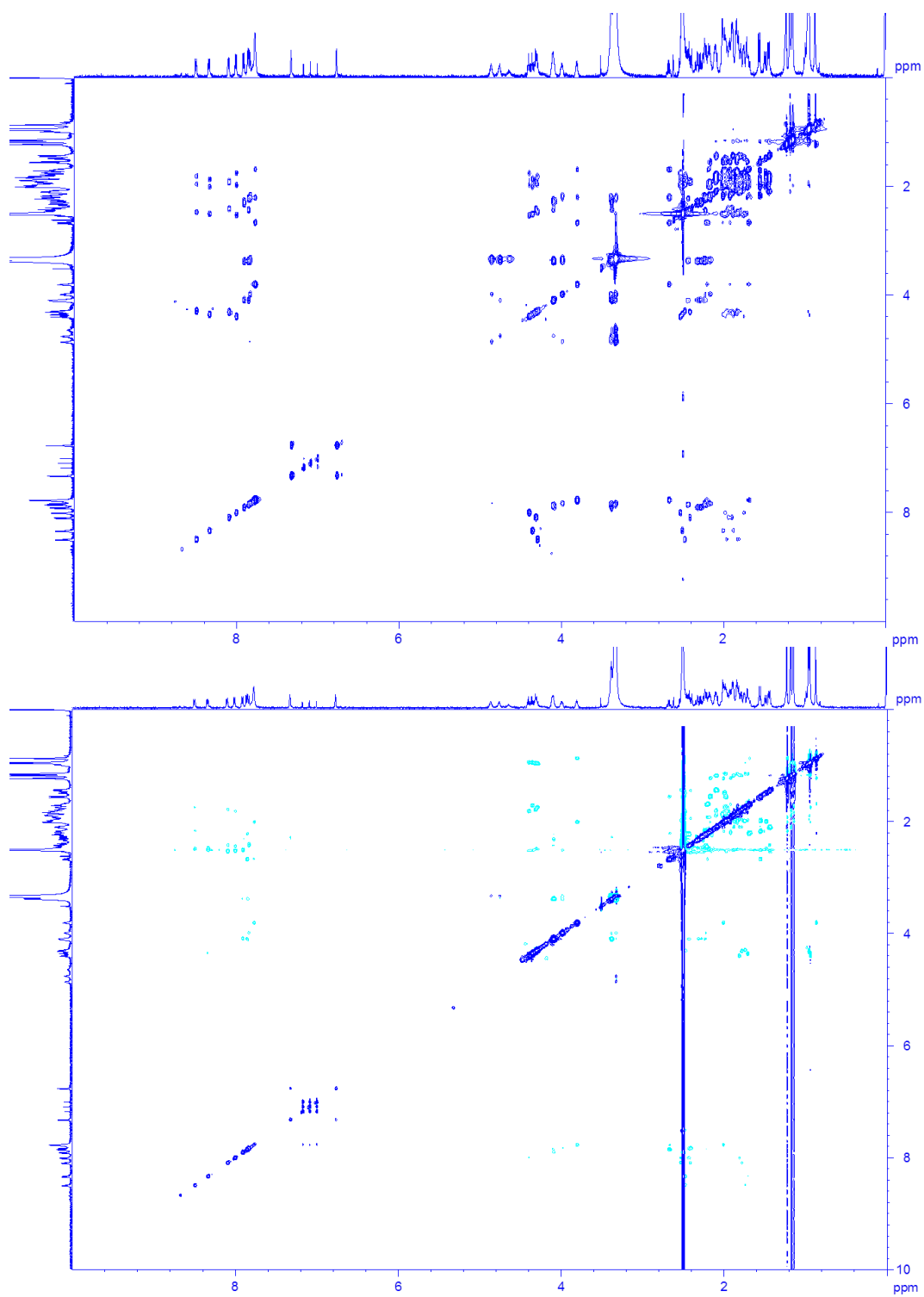


Fig. S4 TOCSY (top) and ROESY (bottom) spectra of **4**. Conditions: [D₆]DMSO, 1 mM, 298 K.

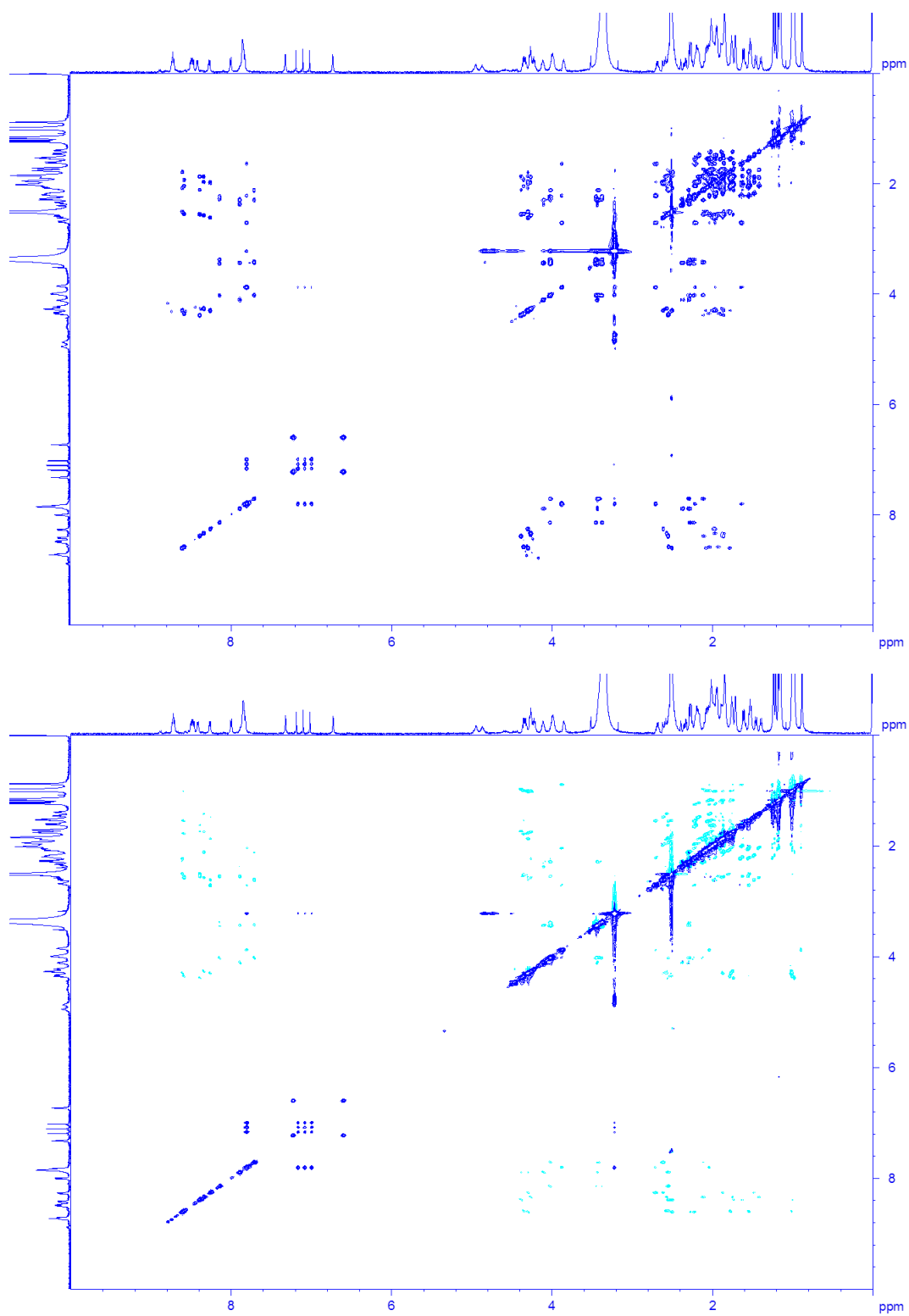


Fig. S5 TOCSY (top) and ROESY (bottom) spectra of **5**. Conditions: [D₆]DMSO, 1 mM, 298 K.

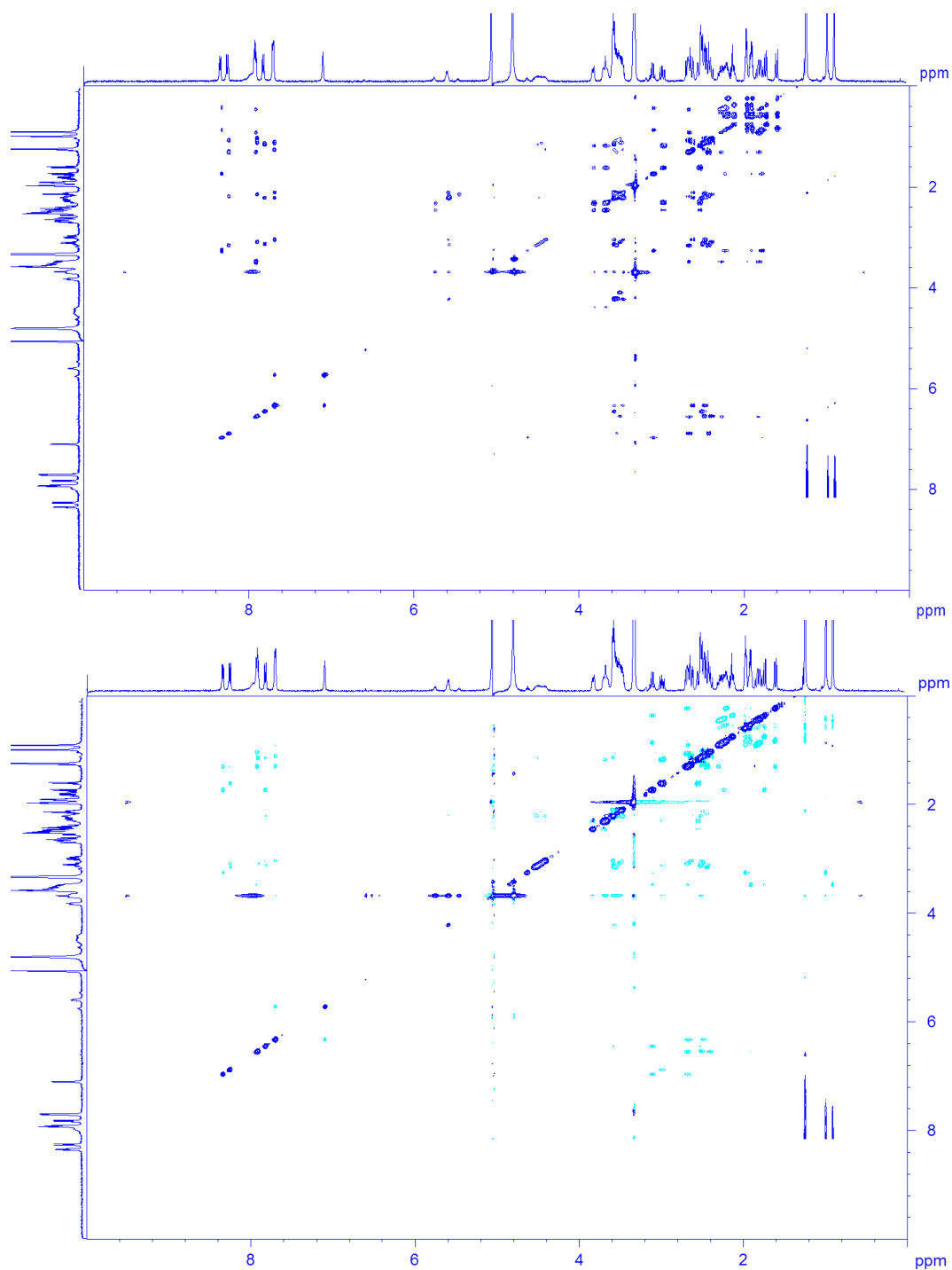


Fig. S6 TOCSY (top) and ROESY (bottom) spectra of **1**. Conditions: CD₃OH, 1 mM, 285 K.

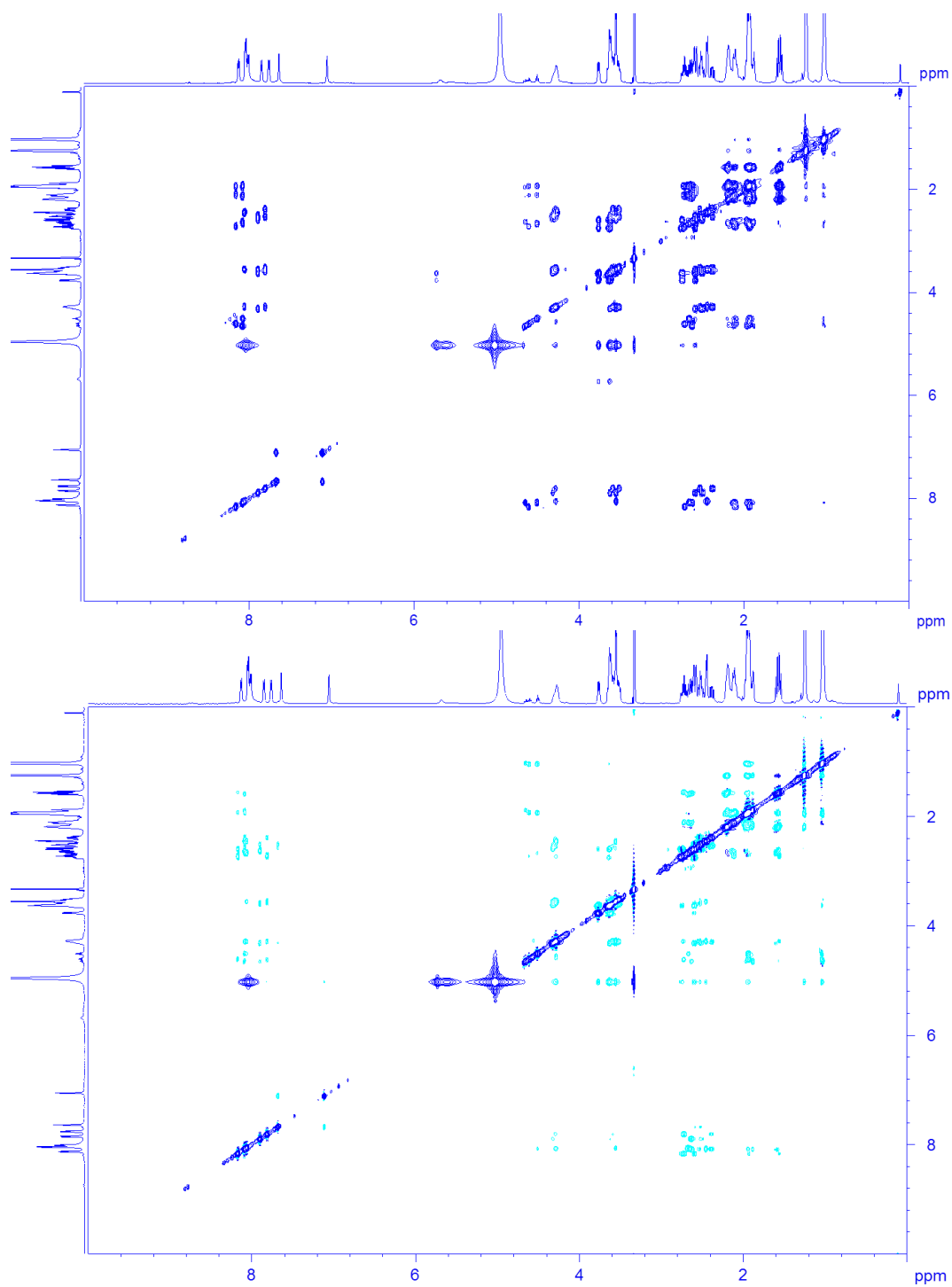


Fig. S7 TOCSY (top) and ROESY (bottom) spectra of **2**. Conditions: CD₃OH, 1 mM, 283 K.

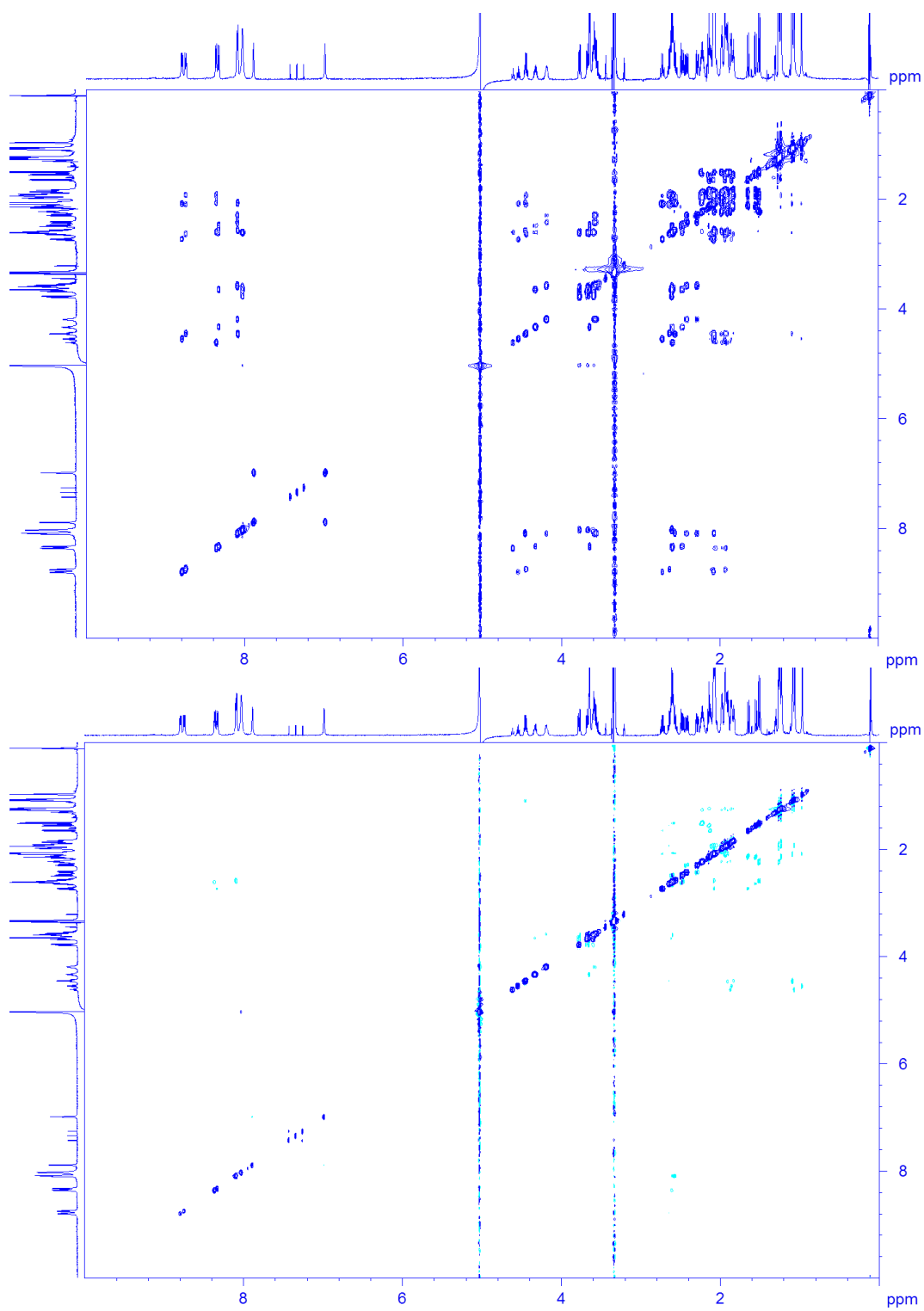


Fig. S8 TOCSY (top) and ROESY (bottom) spectra of **3**. Conditions: CD₃OH, 1 mM, 283 K

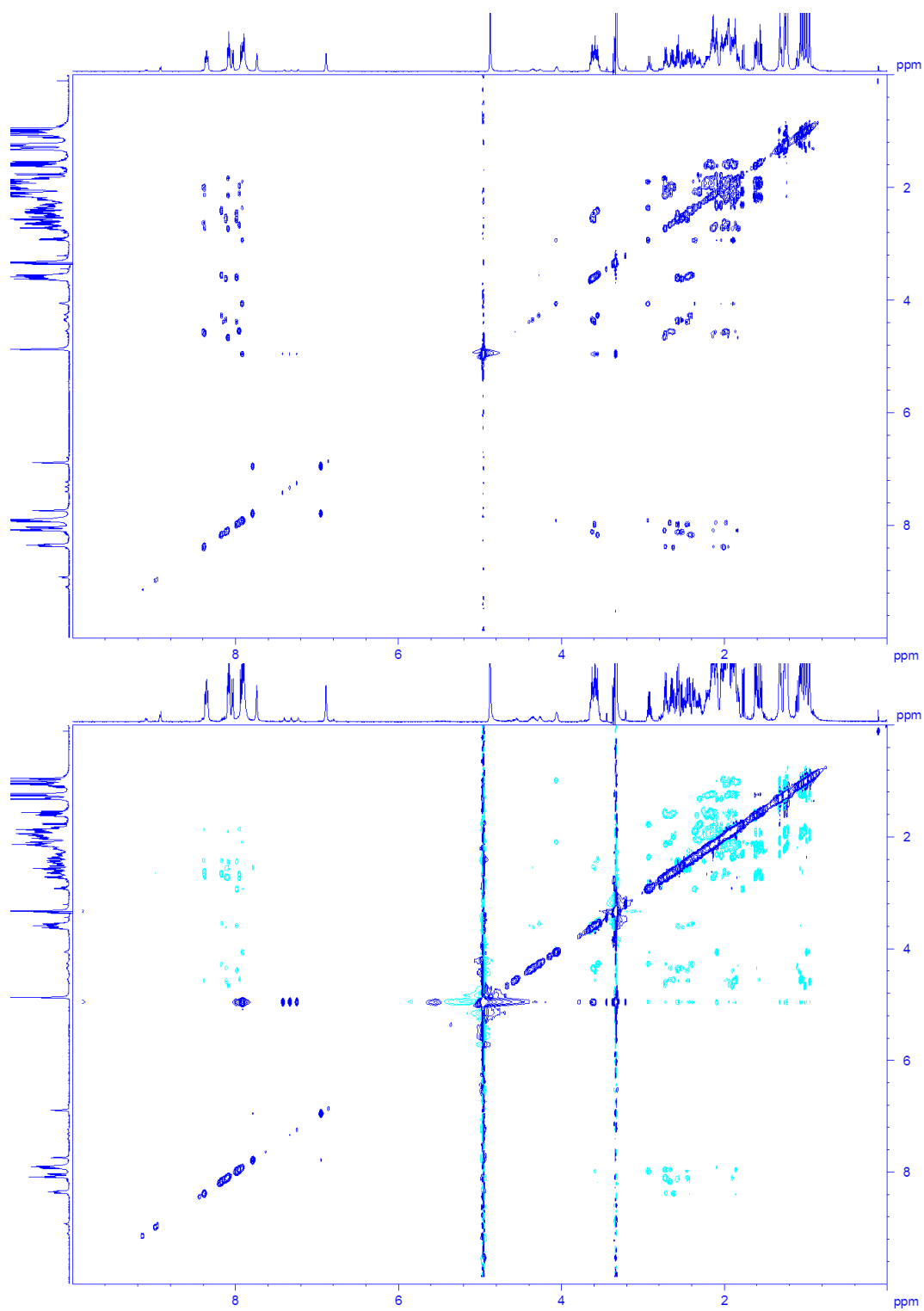


Fig. S9 TOCSY (top) and ROESY (bottom) spectra of **4**. Conditions: CD₃OH, 1 mM, 290 K

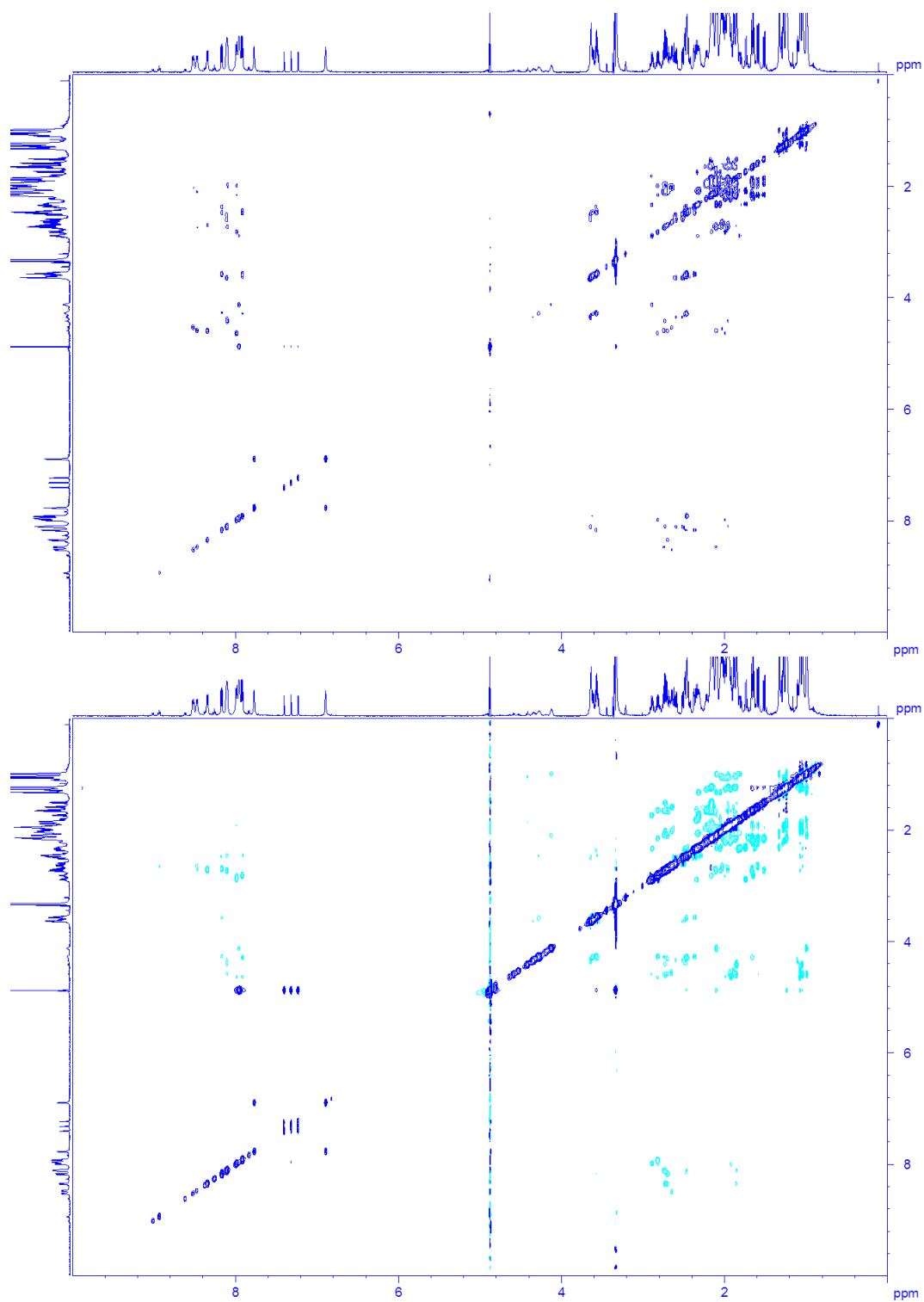


Fig. S10 TOCSY (top) and ROESY (bottom) spectra of **5**. Conditions: CD₃OH, 1 mM, 298 K.

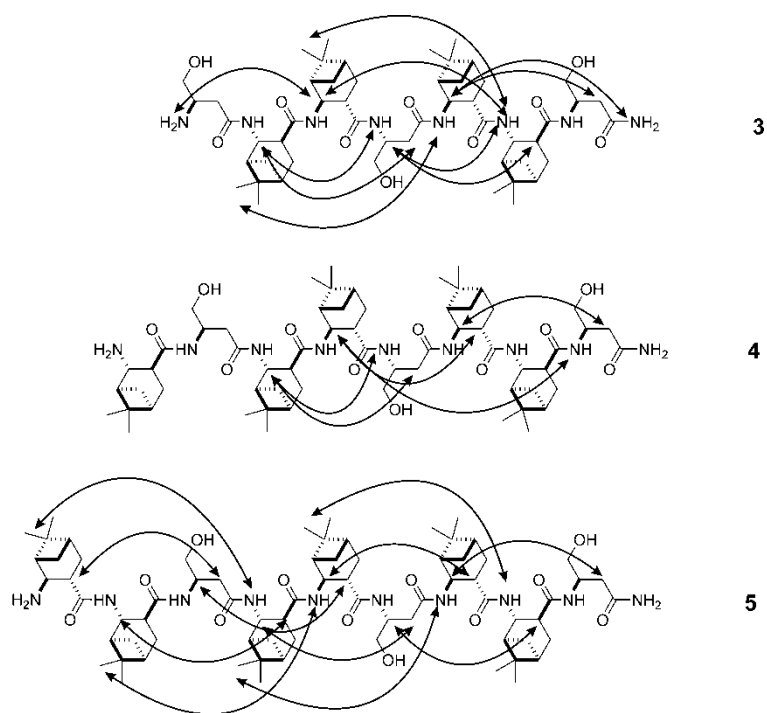


Fig. S11 Long-range NOE interactions for **3-5** in $[D_6]DMSO$.

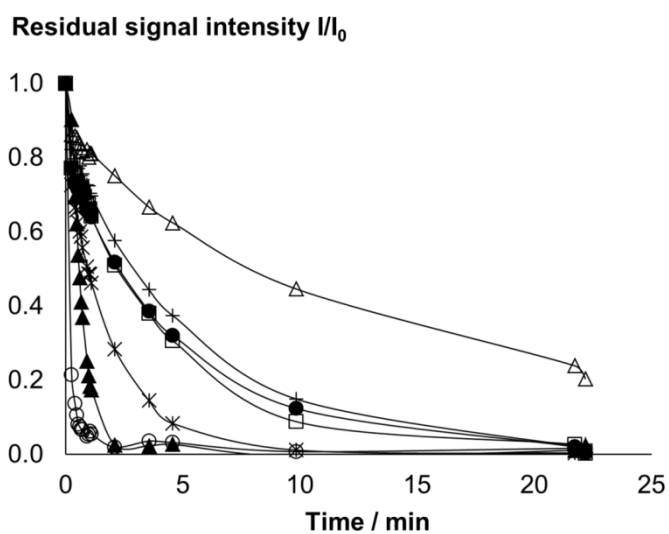


Fig. S12 Time dependence of the NH/ND exchange for **5** in CD_3OD . NH_2-NH_3 (filled triangle); NH_4 (asterisk); NH_5 (empty triangle), NH_6 (plus); NH_7 (filled circle); NH_8 (empty square); NH_9 (empty circle).

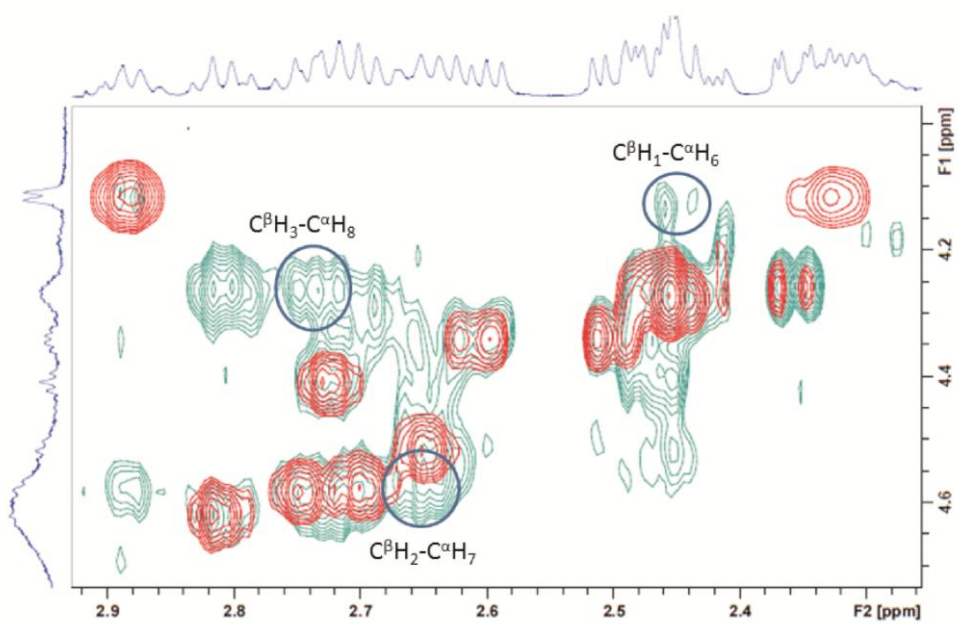


Fig. S13 Diagnostic head-to-tail cross-peaks in the ROESY spectra of **5** in CD₃OH. (red: positive intensity levels, blue: negative intensity levels).

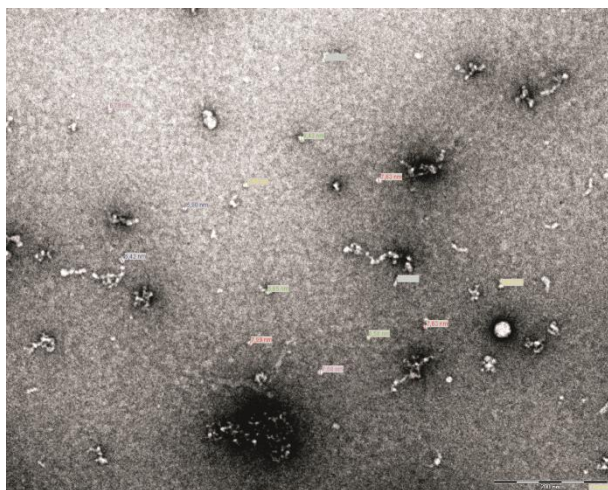


Fig. S14 TEM image of **5**.

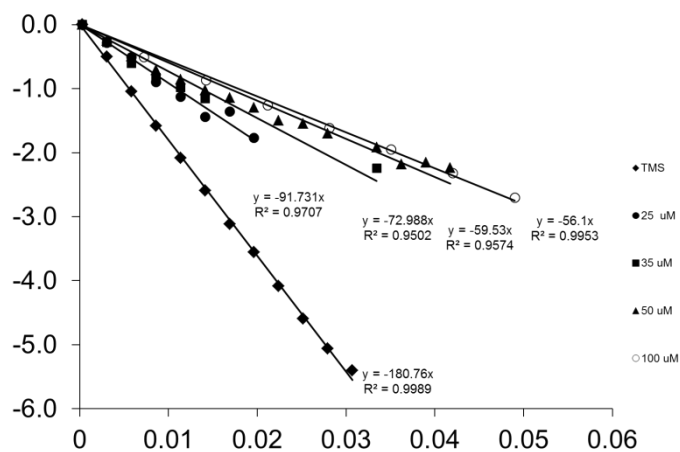


Fig. S15 $\ln(I/I_0)$ vs. G^2 for 3.

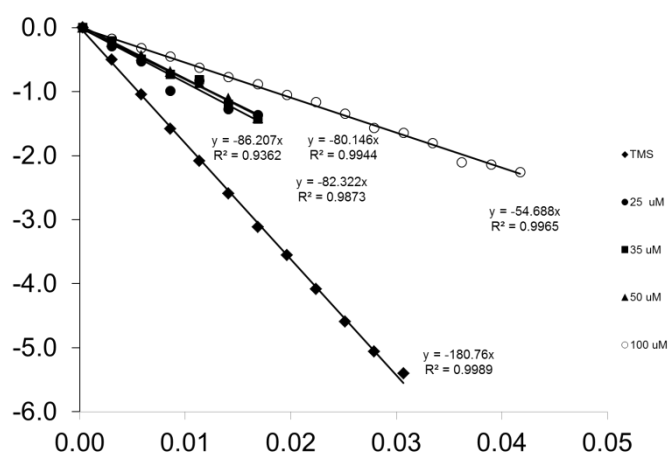


Fig. S16 $\ln(I/I_0)$ vs. G^2 for 4.

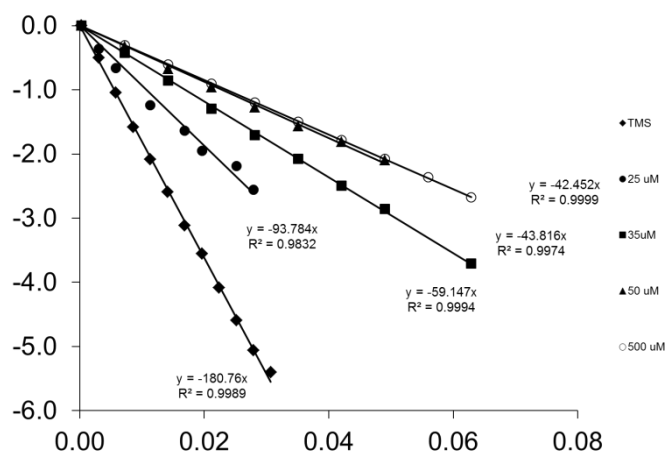


Fig. S17 $\ln(I/I_0)$ vs. G^2 for 5.

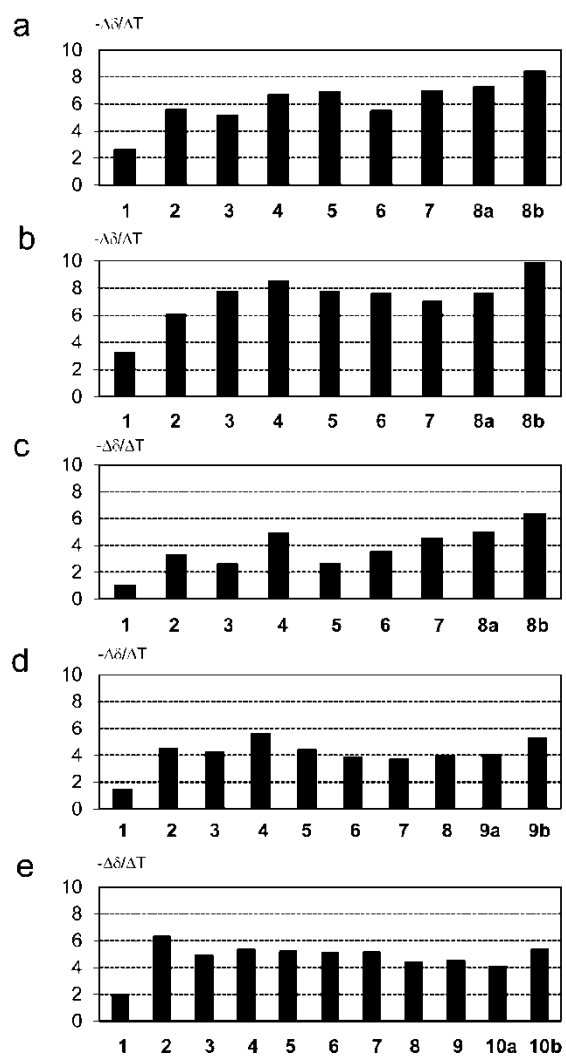


Fig. S18 Negative temperature gradients of the chemical shifts for the NH protons in 1-5 in $[D_6]DMSO$. Panel 1 (a), 2 (b), 3 (c), 4 (d), 5 (e).

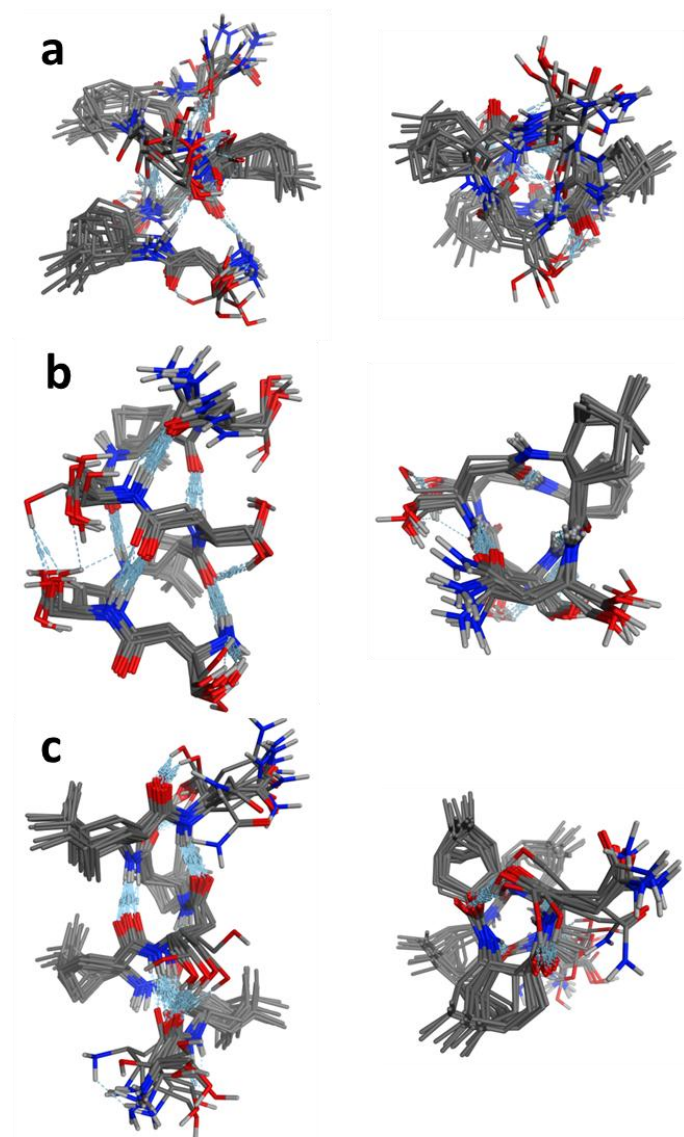


Fig. S19 Ab initio geometries of **1-3**, **a-c** respectively.

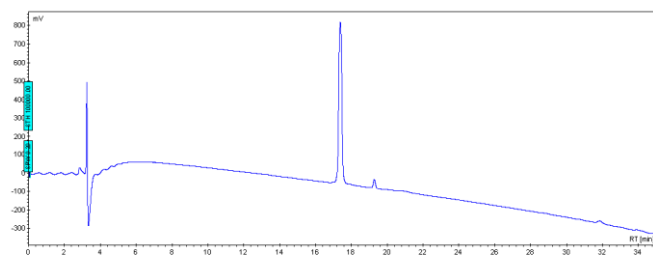


Fig. S20 HPLC chromatogram of purified **1**.

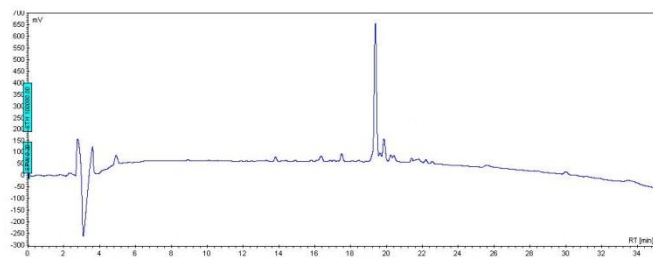


Fig. S21 HPLC chromatogram of purified **2**.

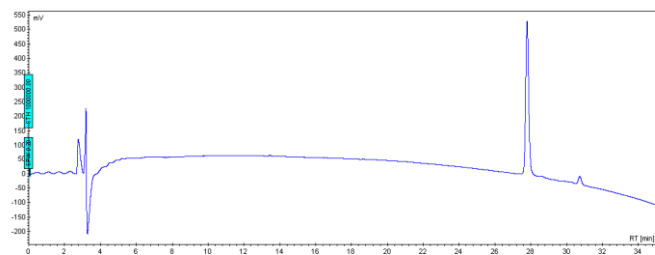


Fig. S22 HPLC chromatogram of purified **3**.

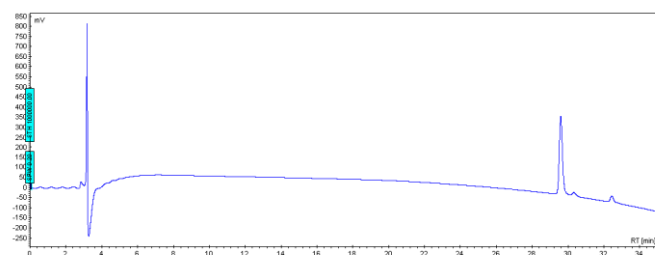


Fig. S23 HPLC chromatogram of purified **4**.

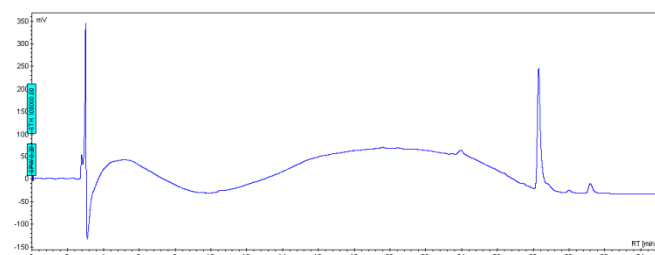


Fig. S24 HPLC chromatogram of purified **5**.

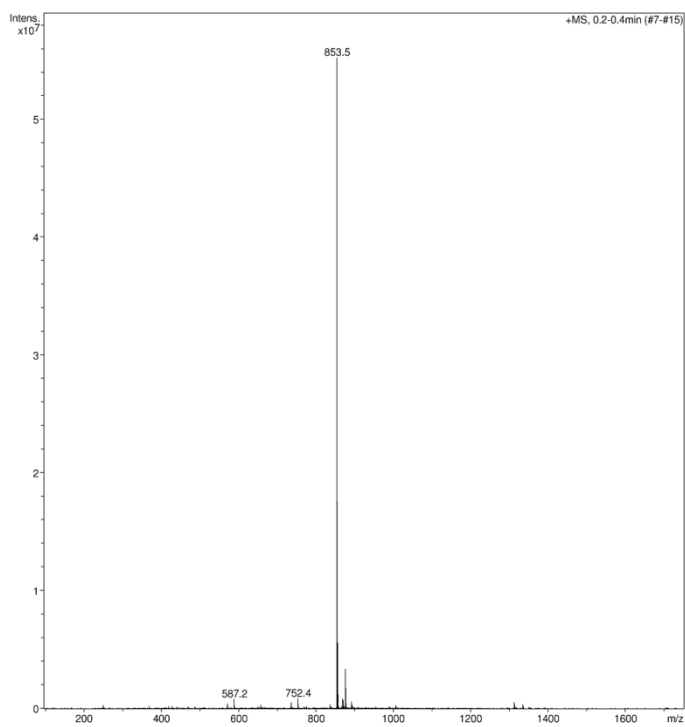


Fig. S25 ESI-MS spectrum of **1**.

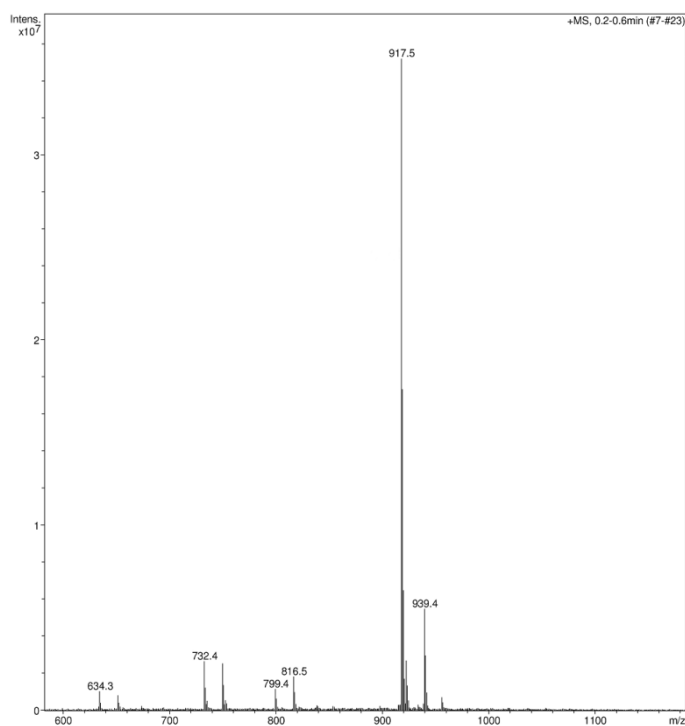


Fig. S26 ESI-MS spectrum of **2**.

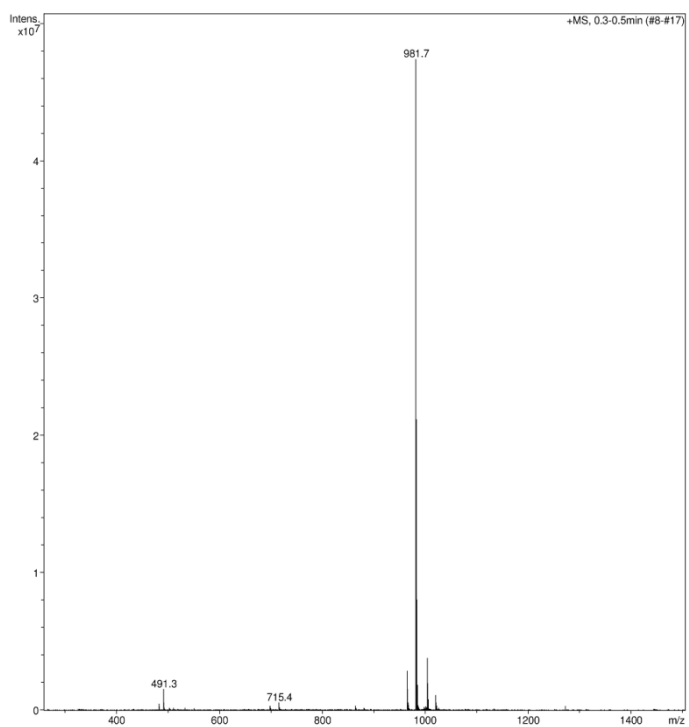


Fig. S27 ESI-MS spectrum of **3**.

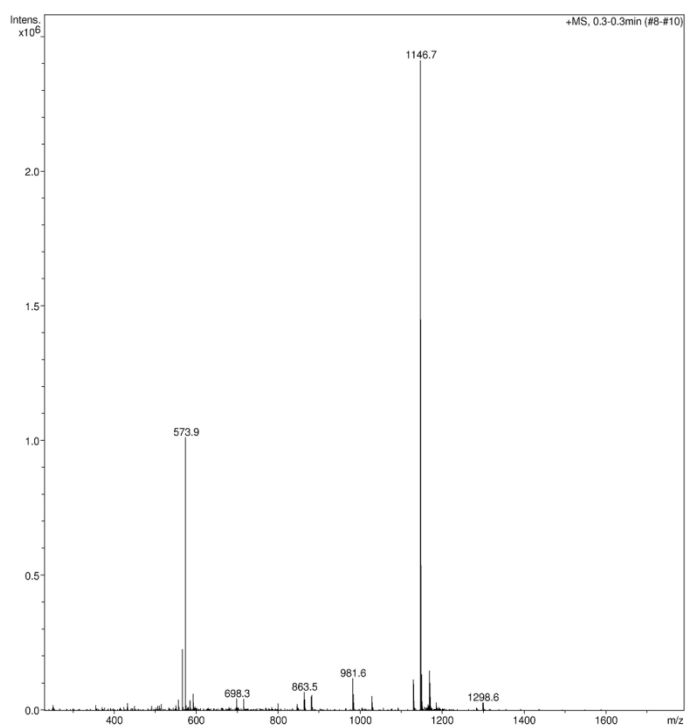


Fig. S28 ESI-MS spectrum of **4**.

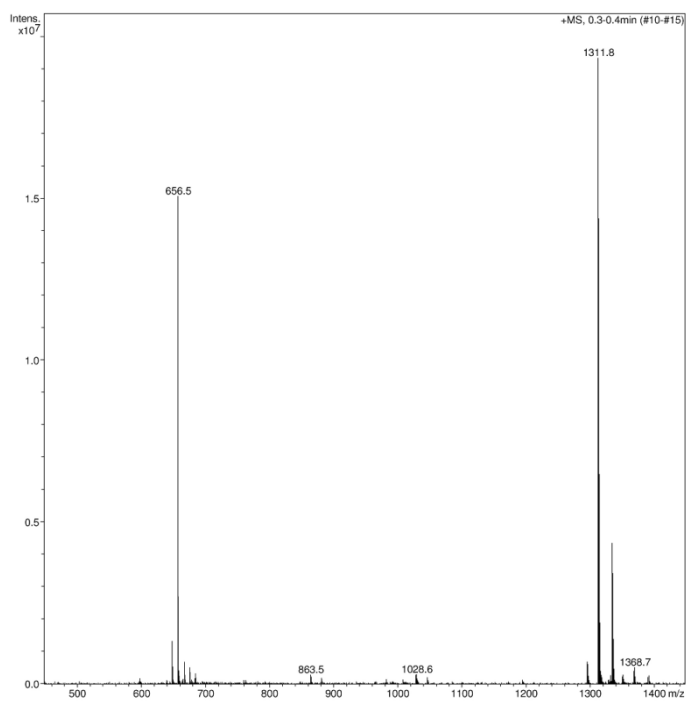


Fig. S29 ESI-MS spectrum of **5**.

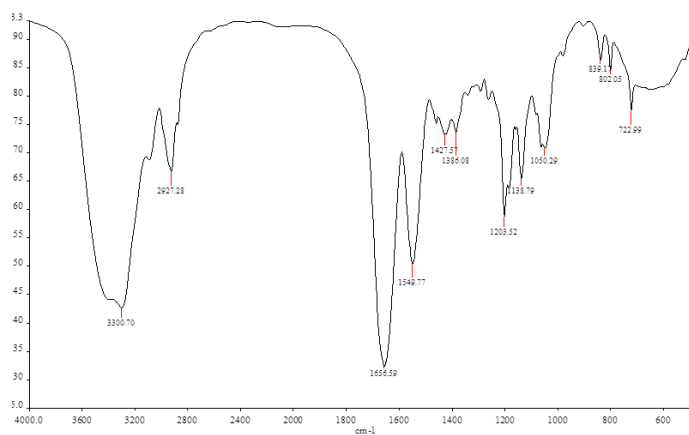


Fig. S30 IR spectrum of **1**.

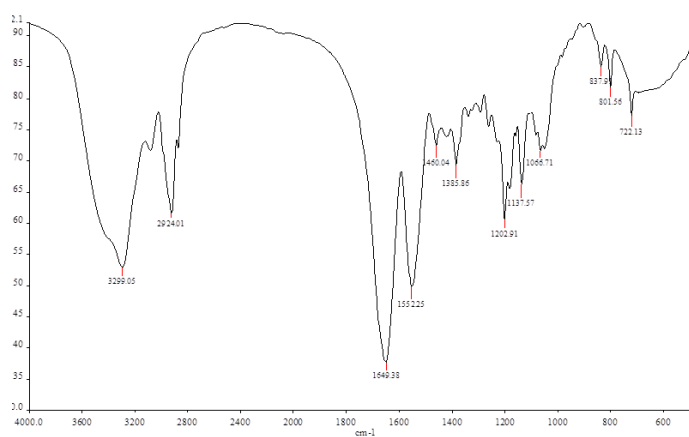


Fig. S31 IR spectrum of **2**.

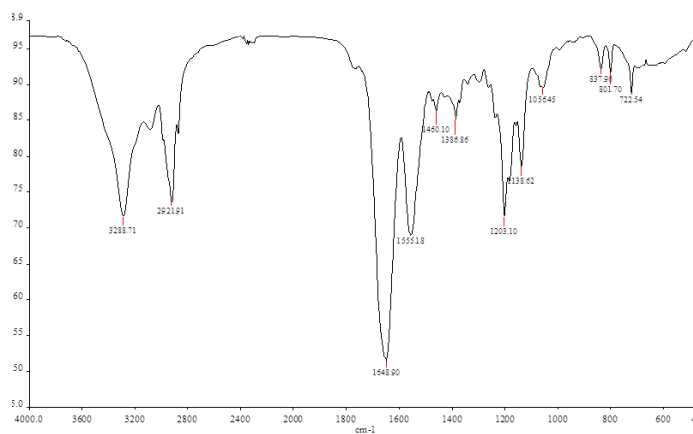


Fig. S32 IR spectrum of **3**.

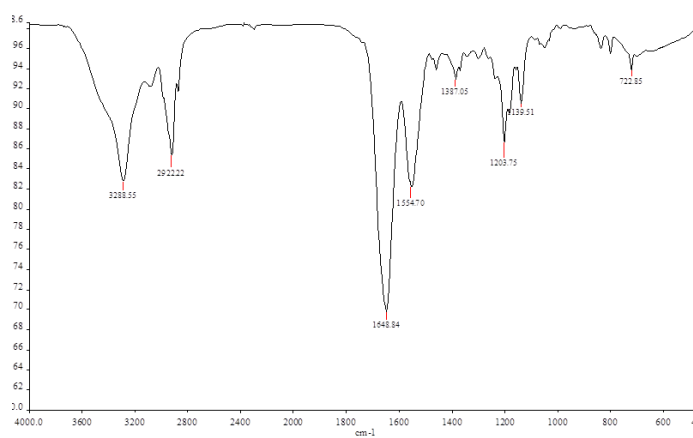


Fig. S33 IR spectrum of **4**.

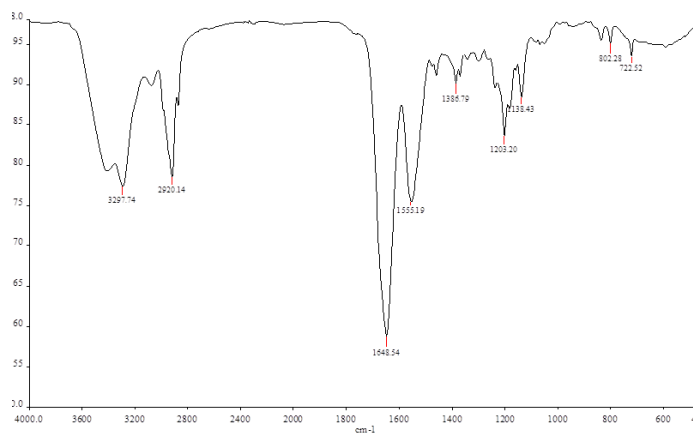


Fig. S34 IR spectrum of **5**.

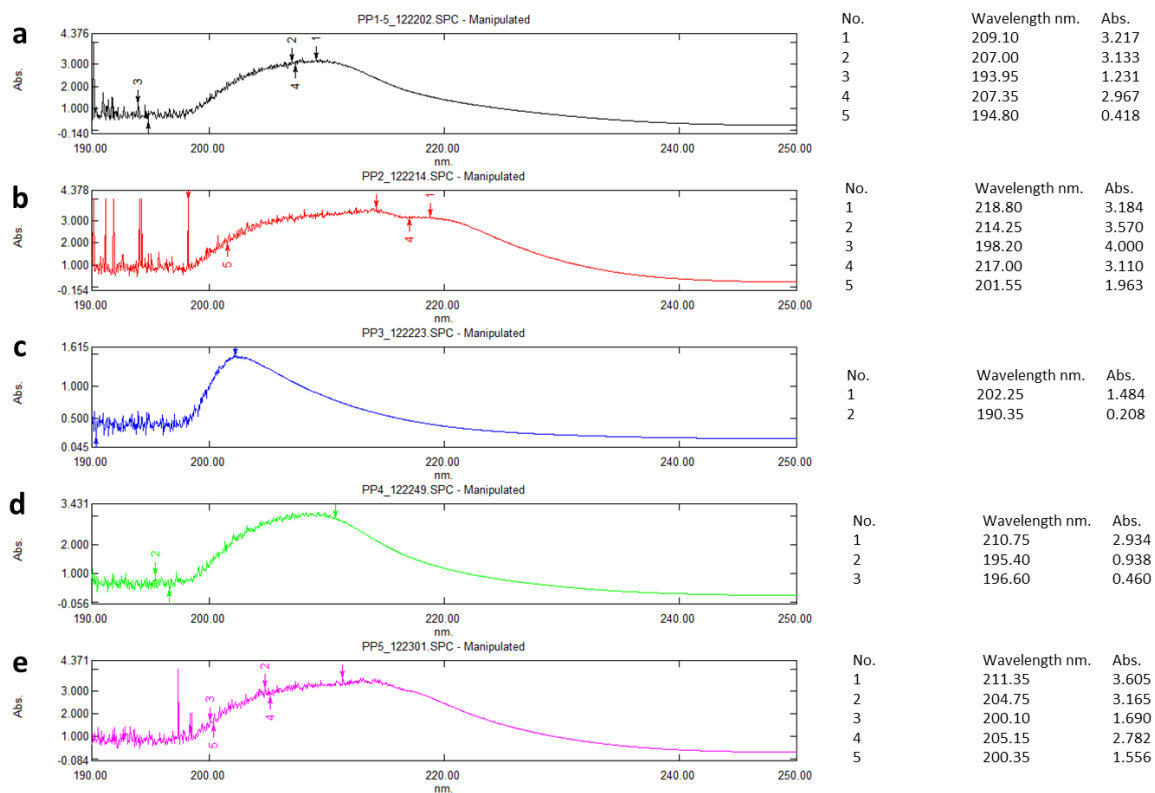


Fig. S35 UV spectra of 1-5, a-e respectively.

Table S1 NMR signal assignment of the backbone for 1-3 in [D₆]DMSO (ppm).

<i>i</i>	1			2			3		
	NH	C _{βi}	C _{αi}	NH	C _{βi}	C _{αi}	NH	C _{βi}	C _{αi}
1	7.76	3.41	2.43	7.79	3.38	2.41	7.77	3.42	2.43
2	7.86	4.11	2.35 2.19	7.98	4.37	2.52	8.12	4.44	2.51
3	7.71	4.38	2.57	7.41	4.03	2.30 2.17	7.92	4.30	2.40
4	7.40	4.06	2.32 2.23	7.75	4.33	2.50	7.67	4.00	2.26 2.14
5	7.63	4.05	2.31 2.23	7.54	4.02	2.24	8.44	4.31	2.48
6	7.73	4.39	2.52	7.77	4.35	2.50	8.32	4.37	2.54
7	7.44	4.05	2.30 2.30	7.43	4.02	2.31 2.25	7.91	4.11	2.32
8				7.28 6.77			7.33 6.77		

Table S2 NMR signal assignment of the backbone for **4-5** in [D₆]DMSO (ppm).

<i>i</i>	4			5		
	NH	C _{βi}	C _{αi}	NH	C _{βi}	C _{αi}
1	7.77	3.80	2.66	7.80	3.88	2.70
2	7.85	4.09	2.43 2.23	8.26	4.30	2.61
3	8.00	4.39	2.53	7.71	4.02	2.11
4	8.09	4.31	2.41	8.34	4.26	2.57
5	7.83	3.98	2.20 2.17	8.58	4.35	2.55
6	8.49	4.29	2.47	8.14	4.02	2.23
7	8.33	4.35	2.51	8.60	4.30	2.51
8	7.90	4.09	2.30	8.39	4.38	2.55
9	7.32 6.76			7.89	4.10	2.29
10						

Table S3 NMR signal assignment of the backbone for **1-3** in CD₃OH (ppm).

<i>i</i>	1			2			3		
	NH	C _{βi}	C _{αi}	NH	C _{βi}	C _{αi}	NH	C _{βi}	C _{αi}
1	8.06	3.65	2.75 2.60			3.00	8.03	3.59	2.60
2	8.16	4.61	2.72	8.26	4.53	2.69 2.45	8.36	4.61	2.60
3	7.81	4.28	2.54 2.39	8.35	4.64	3.12	8.08	4.46	2.58
4	8.08	4.51	2.66	7.83	4.51	2.53	8.09	4.19	2.42 2.29
5	8.06	4.28	2.45	7.92	4.47	2.49 2.42	8.75	4.44	2.63
6	8.08	4.65	2.63	7.94	4.86	2.69	8.79	4.55	2.73
7	7.89	4.32	2.60 2.51	7.71	4.43	2.64 2.49	8.33	4.32	2.60 2.47
8	7.68			7.71 7.10			7.89 6.98		

Table S4 NMR signal assignment of the backbone for **4-5** in CD₃OH (ppm).

<i>i</i>	4			5		
	NH	C _{βi}	C _{αi}	NH	C _{βi}	C _{αi}
1	7.92	4.07	2.94	7.95	4.12	2.88
2	7.99	4.38	2.57 2.45	8.02	4.63	2.82
3	8.09	4.66	2.73	7.93	4.28	2.47
4	7.95	4.55	2.67	8.13	4.41	2.73
5	8.17	4.28	2.42	8.39	4.59	2.69
6	8.39	4.57	2.62	8.19	4.26	2.47
7	8.37	4.59	2.72	8.57	4.53	2.64
8	8.12	4.35	2.55	8.52	4.58	2.74
9	7.79			8.15	4.37	2.60
10						

Table S5. ³*J* (NH_{*i*}- C^βH_{*i*}) values in [D₆]DMSO.

<i>i</i>	1	2	3	4	5
2	8.05	8.52	8.21	8.53	7.82
3	8.93	8.45	7.76	8.17	7.99
4	8.37	8.24	8.29	8.06	9.04
5	8.16	8.49	8.89	8.43	8.97
6	8.37	8.02	8.69	8.56	8.31
7	8.79	8.40	8.29	8.87	9.07
				8.19	9.05
8					8.18
9					

Table S6. ³*J* (NH_{*i*}- C^βH_{*i*}) values in CD₃OH.

<i>i</i>	1	2	3	4	5
2	8.01	8.99	8.28	8.67	8.10
3	8.55	7.30	8.22	8.22	8.27
4	8.34	9.07	8.16	8.36	8.49
5	8.61	8.50	9.23	8.42	8.45
6	8.74	8.35	9.18	7.80	8.38
7	8.44	7.33	8.54	6.99	8.34
				8.33	8.34
8					9.02
9					

Table S7. Measured aggregation numbers (N) for 3-5.

3	Calculated volume	Calculated radius	Diffusion constant	Measured radius	Aggregation number
	Å ³	Å	×10 ⁻⁹ m ² s ⁻¹	Å	N
TMS ^a	409.42	4.20	2.53	4.20	1.00
25 μM	2437.19	8.20	1.29	8.28	1.03
35 μM	2437.19	8.20	1.02	10.40	2.04
50 μM	2437.19	8.20	8.34	12.75	3.76
100 μM	2437.19	8.20	7.86	13.53	4.49

4	Calculated volume	Calculated radius	Diffusion constant	Measured radius	Aggregation number
	Å ³	Å	×10 ⁻⁹ m ² s ⁻¹	Å	N
TMS ^a	409.42	4.20	2.53	4.20	1.00
25 μM	2437.19	8.30	1.26	8.46	1.06
35 μM	2437.19	8.30	1.15	9.22	1.37
50 μM	2437.19	8.30	1.12	9.47	1.78
100 μM	2437.19	8.30	7.68	13.85	4.65

5	Calculated volume	Calculated radius	Diffusion constant	Measured radius	Aggregation number
	Å ³	Å	×10 ⁻⁹ m ² s ⁻¹	Å	N
TMS ^a	113.25	4.20	2.53	4.61	1.00
25 μM	2482.71	8.40	1.31	9.28	0.86
35 μM	2482.71	8.40	8.29	10.11	3.68
50 μM	2482.71	8.40	6.14	10.39	8.78
100 μM	2482.71	8.40	5.96	15.19	9.18

^aexternal reference

M. J. Frisch, G. W. Trucks, H. B. Schlegel, G. E. Scuseria, M. A. Robb, J. R. Cheeseman, G. Scalmani, V. Barone, B. Mennucci, G. A. Petersson, H. Nakatsuji, M. Caricato, X. Li, H. P. Hratchian, A. F. Izmaylov, J. Bloino, G. Zheng, J. L. Sonnenberg, M. Hada, M. Ehara, K. Toyota, R. Fukuda, J. Hasegawa, M. Ishida, T. Nakajima, Y. Honda, O. Kitao, H. Nakai, T. Vreven, J. A. Montgomery, Jr., J. E. Peralta, F. Ogliaro, M. Bearpark, J. J. Heyd, E. Brothers, K. N. Kudin, V. N. Staroverov, R. Kobayashi, J. Normand, K. Raghavachari, A. Rendell, J. C. Burant, S. S. Iyengar, J. Tomasi, M. Cossi, N. Rega, J. M. Millam, M. Klene, J. E. Knox, J. B. Cross, V. Bakken, C. Adamo, J. Jaramillo, R. Gomperts, R. E. Stratmann, O. Yazyev, A. J. Austin, R. Cammi, C. Pomelli, J. W. Ochterski, R. L. Martin, K. Morokuma, V. G. Zakrzewski, G. A. Voth, P. Salvador, J. J. Dannenberg, S. Dapprich, A. D. Daniels, Ö. Farkas, J. B. Foresman, J. V. Ortiz, J. Cioslowski, and D. J. Fox, Gaussian, Inc., Wallingford CT, 2009.